Thermochimica Acta 503–504 (2010) 21–27

Contents lists available at ScienceDirect

Thermochimica Acta

journal homepage: www.elsevier.com/locate/tca

Thermal analysis of manganese(II) complexes of general formula $(Et_4N)_2[MnBr_nCl_{4-n}]$

E. Styczeń [a], M. Gazda [b], D. Wyrzykowski [a,*]

[a] Faculty of Chemistry, University of Gdańsk, Sobieskiego 18, 80-952 Gdańsk, Poland
[b] Faculty of Physics and Mathematics, Technical University of Gdańsk, Narutowicza 11/12, 80-952 Gdańsk, Poland

ARTICLE INFO

Article history:
Received 18 January 2010
Received in revised form 25 February 2010
Accepted 1 March 2010
Available online 6 March 2010

Keywords:
Tetrahalogenomanganates(II)
Thermal decomposition
DSC

ABSTRACT

Thermal decomposition of compounds consisting of tetrahalogenomanganates(II) anions, $[MnBr_nCl_{4-n}]^{2-}$ (n = 0–4), and a tetraethylammonium cation has been studied using the DSC and TG techniques. The measurements were carried out in an argon atmosphere over the temperature ranges 173–500 K (DSC) and 300–1073 K (TG). Products of the thermal decomposition were identified by MS, FTIR, Far-FTIR spectroscopy as well as X-ray powder diffractometry.

1. Introduction

In 1992, Peter Day and associates from the University College, London, published the first report on utilization of the $(BEDT\text{-}TTF)_2CuCl_4{\cdot}H_2O$ compounds as magnetic molecular conductors [1]. Successive investigations have shown that these systems, owing to interaction of alternate organic–inorganic sheets have interesting physical properties such as superconductivity [2–4]. In respect of high-spin configurations of *d* electrons, the inorganic sheet in the conductors can be formed by paramagnetic complex anions of general formula $[MX_4]^{n-}$ where M = Mn, Fe, Co, Ni, Cu; X = Cl, Br; n = 1, 2. As such, tetraalkylammonium salts of tetrahalogenometallates(II) have been subsequently used to synthesize those compounds [1,5–10]. The complexes constitute thus an exciting area of exploration aimed principally at elucidation of their structure as well as magnetic and spectroscopic properties including infrared spectra (FTIR and Far-FTIR), reflection spectra, and EPR. From the point of view of application of the magnetic molecular conductors interesting are also their as yet poorly explored thermal characteristics. Stability characteristics of the systems at various temperatures may be useful for designing magnetic molecular conductors. Furthermore, knowledge of their thermal decomposition products may be helpful for working out procedures for utilization of appliances containing the conductors.

This contribution is a continuation of our studies on thermal analysis of bis(tetraalkylammonium) tetrahalogenometallates(II) [11–14]. Knowledge of thermal characteristics of a large group of compounds would enable to determine the influence of the organic cation, the metal and the halide ligand on thermal stability of compounds with an $[MX_4]^{n-}$ anion.

2. Experimental

2.1. Synthesis

The manganese(II) complex salts were obtained by a procedure described in the literature, by mixing together stoichiometric quantities of a manganese(II) halide with tetraethylammonium chloride and/or bromide in ethanol [15].

$(Et_4N)_2[MnCl_4]$. $MnCl_2$ (0.05 mol) was dissolved in a small quantity of ethanol and the solution was added to ethanolic solution of Et_4NCl (0.1 mol). (Found: C, 42.02; N, 6.11; H, 8.98. Calcd. for $(Et_4N)_2[MnCl_4]$, C, 42.03; N, 6.13; H, 8.82%).

$(Et_4N)_2[MnBr_4]$ was also prepared as described, by using $MnBr_2$ (0.05 mol) and Et_4NBr. (Found: C, 30.35; N, 4.39; H, 6.32. Calcd. for $(Et_4N)_2[MnBr_4]$, C, 30.26; N, 4.41; H, 6.35%).

$(Et_4N)_2[MnBrCl_3]$. $MnCl_2$ (0.05 mol) was dissolved in a small quantity of ethanol and the solution was added to an equimolar mixture (0.05 mol each) of Et_4NCl and Et_4NBr in ethanol. (Found: C, 38.89; N, 5.74; H, 8.31. Calcd. for $(Et_4N)_2[MnBrCl_3]$, C, 38.30; N, 5.58; H, 8.04%).

$(Et_4N)_2[MnBr_3Cl]$ was prepared as described, but $MnBr_2$ (0.05 mol) was used as a manganese halide. (Found: C, 32.78; N, 4.79; H, 7.02. Calcd. for $(Et_4N)_2[MnBr_3Cl]$, C, 32.54; N, 4.74; H, 6.83%).

* Corresponding author. Tel.: +48 523 53 94.
E-mail address: daro@chem.univ.gda.pl (D. Wyrzykowski).

0040-6031/$ – see front matter © 2010 Elsevier B.V. All rights reserved.
doi:10.1016/j.tca.2010.03.001

$(Et_4N)_2[MnBr_2Cl_2]$. $MnCl_2$ (0.05 mol) was dissolved in a small quantity of ethanol and the solution was added to an ethanolic solution of Et_4NBr (0.01 mol). (Found: C, 35.25; N, 5.27; H, 7.52. Calcd. for $(Et_4N)_2[MnBr_2Cl_2]$, C, 35.19; N, 5.13; H, 7.38%).

2.2. Instrumental

The Far-FTIR spectra were recorded on a BRUKER IFS 66 spectrophotometer in PE over the 650–50 cm^{-1} range.

The DSC measurements were carried out in an argon (Ar 5.0) on a *NETZSCH DSC 204* apparatus (range 173–500 K, aluminum crucible, sample mass *ca.* 10 mg, heating rate 10 K/min).

The TG-FTIR analyses in argon (Ar 5.0) were run on a Netzsch TG 209 apparatus coupled with a Bruker FTIR IFS66 spectrophotometer (range 298–1073 K, corundum crucible, sample mass *ca.* 12 mg, heating rate 15 K/min, flow rate of the carrier gas 18 mL/min).

The TG–MS measurements in argon were carried out on a Netzsch STA 449 F3 Jupiter apparatus (TA Instruments) (range 290–1273 K, corundum crucible, sample mass *ca.* 5–10 mg, heating rate 1–10 K/min). The thermal analysis instrument was connected on-line with the quadrupole mass spectrometer QMS 403C Aëolos.

The course of thermal analysis was broken at points corresponding to the main steps of decomposition and the residues in the crucible were quickly cooled in the stream of argon. This enabled to analyze the residues at strictly pre-determined steps of decomposition. The analysis was carried out using the FTIR spectroscopic techniques as well as the X-ray powder diffractometry.

The presence of crystalline phases was checked by X-ray diffraction with the use of Philips X'Pert diffractometer system. The XRPD patterns were recorded at room temperature with CuK_α radiation (λ = 1.540 Å). Qualitative analysis of the diffraction spectra was carried out with the ICDD PDF database [16].

3. Results and discussion

Results of the thermal analysis of the complexes are compiled in Tables 1 and 2.

There are no changes in the DSC curve of $(Et_4N)_2[MnCl_4]$ upon raising temperature up to that close to the decomposition point (573 K). They emerge only upon cooling the sample down to 173 K. Peaks appearing at 221 and 189 K are assigned to reversible exothermic transformations. They origin can be attributed to small movements of the ions resulting in the change of their mutual position. As a consequence, parameters of the elementary cell of $(Et_4N)_2[MnCl_4]$ can be changed as was the case with $(Me_4N)_2[MnCl_4]$ [17].

The $(Et_4N)_2[MnBrCl_3]$, $(Et_4N)_2[MnBr_2Cl_2]$ and $(Et_4N)_2[MnBr_4]$ complexes (Fig. 1), upon heating up to their decomposition points (*ca.* 523 K) (heating 1), undergo reversible endothermic phase transformations, most probably owing to transformation of one polymorphic form to another. Upon cooling of the compound down to 173 K (cooling 1), a peak below 273 K appears in the DSC curve assigned to another phase transformation that is also reversible as demonstrated by a peak at similar temperature and of similar surface area recorded upon reheating the sample (heating 2). As in the case of $(Et_4N)_2[MnCl_4]$, the transformation could also be attributed to small movements of the ions. The DSC curves of $(Et_4N)_2[MnBr_4]$ recorded upon heating the sample from ambient temperature up to 500 K (heating 1) followed by its cooling down to 173 K (cooling 1) and reheating up to 500 K (heating 2) are shown in Fig. 1.

The greatest number of transformations occurring upon changes of temperature among the bis(tetraethylammonium) tetrahalogenmanganates(II) was noticed with $(Et_4N)_2[MnBr_3Cl]$. Apart from analogous ones recorded with $(Et_4N)_2[MnBrCl_3]$, $(Et_4N)_2[MnBr_2Cl_2]$ and $(Et_4N)_2[MnBr_4]$, such as the reversible endothermic one occurring upon heating the sample, and the reversible exothermic one upon cooling, an additional peak emerges at 389 K assignable to irreversible endothermic transformation. Its origin is based on lack of a similar peak upon reheating the sample (heating 2, Fig. 2).

A common feature of the $(Et_4N)_2[MnBr_nCl_{4-n}]$ compounds is their thermal dissociation occurring in the solid state. This means that they have no melting point prior to decomposition.

Table 1
Temperature and enthalpy changes for physical transformations of the manganese(II) complex as taken from the DCS curve.

Complexes	T_σ (K)	ΔH_σ (kJ/mol)
$(Et_4N)_2[MnCl_4]$	221^R	−3.2
	189^R	−4.4
$(Et_4N)_2[MnBrCl_3]$	462^R	1.7
	222^R	−2.5
$(Et_4N)_2[MnBr_2Cl_2]$	432^R	2.5
	236^R	−2.8
$(Et_4N)_2[MnBr_3Cl]$	389^I	8.1
	430^R	2.3
	260^R	−3.3
$(Et_4N)_2[MnBr_4]$	443^R	11.0
	255^R	−4.6

T_σ: temperature of phase transformation; ΔH_σ: enthalpy of phase transformation; R: reversible; I: irreversible.

Table 2
Results of analysis of the decomposition products.

Complex	Step	Temp. range (K)	DTG_{min} (K)	Mass loss (%)
$(Et_4N)_2[MnCl_4]$	1	573–643	599	61
	2	643–688	665	11
	3	858–968		12
$(Et_4N)_2[MnBrCl_3]$	1[a]	553–693	601	66
	2	733–943		16
$(Et_4N)_2[MnBr_2Cl_2]$	1	548–628	585	56
	2	628–683	639	10
	3	728–866		20
$(Et_4N)_2[MnBr_3Cl]$	1	563–608	584	36
	2	608–658	636	25
	3	758–958		26
$(Et_4N)_2[MnBr_4]$	1	538–603	583	35
	2	603–653	633	25
	3	763–983	968	30

[a] Split into steps at a slower rise in temperature.

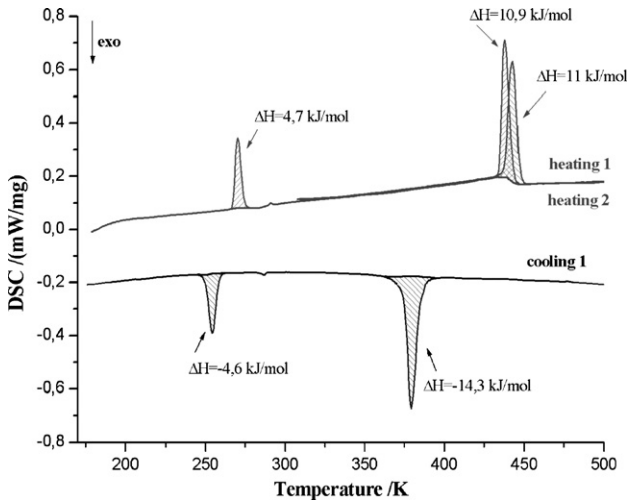

Fig. 1. DSC curves of $(Et_4N)_2[MnBr_4]$, β = 10 K/min.

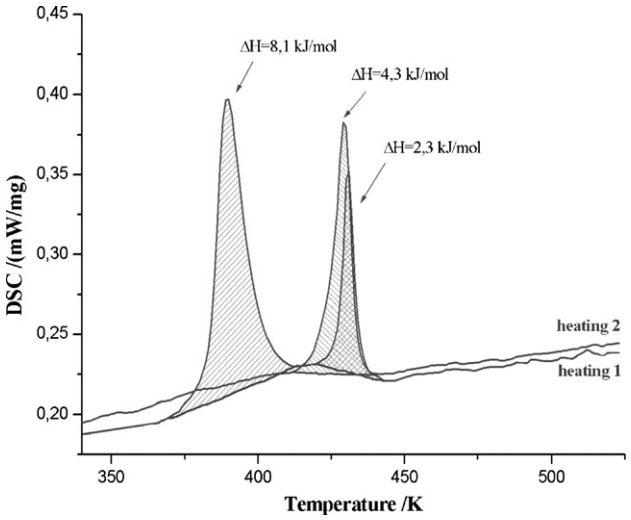

Fig. 2. DSC curves of $(Et_4N)_2[MnBr_3Cl]$, $\beta = 10$ K/min.

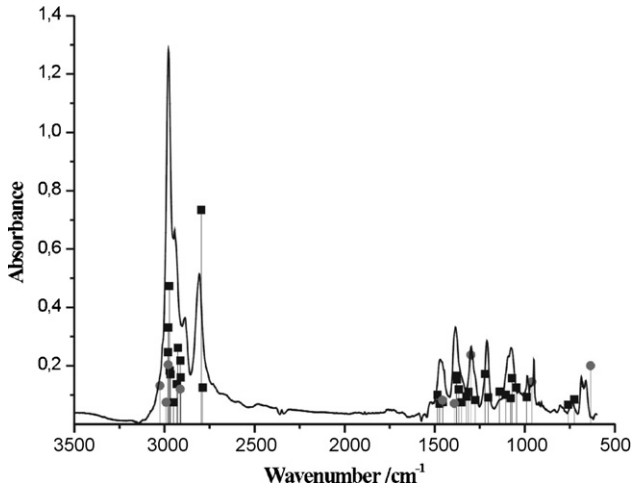

Fig. 4. FTIR spectrum of the volatile decomposition products of $(Et_4N)_2[MnCl_4]$, at 630 K, together with theoretical harmonic transitions for Et_3N (squares) and EtCl (circles) [18].

A closer inspection of the results of the thermal decomposition of bis(tetraethylammonium) tetrahalogenomanganates(II) reveals the influence of anion identity on the pathways of their thermal dissociation. The differences lie in the formation of various solids during the first step.

In spite of the differences in the solids' composition, similar volatile products are released. For instance, upon heating of $(Et_4N)_2[MnCl_4]$, Et_3N and EtCl are released (Fig. 3), whereas in the case of $(Et_4N)_2[MnBr_4]$–Et_3N and EtBr. Fig. 3 represents a TG curve of an exemplary compound, $(Et_4N)_2[MnCl_4]$, with superimposed curves of ionic currents for selected m/z values corresponding to EtCl {m/z = 26 ($C_2H_2^+$), 27 ($C_2H_3^+$), 28 ($C_2H_4^+$), 29 ($C_2H_5^+$), 49 (CH_2Cl^{35+}), 64 ($C_2H_5Cl^{35+}$) and 66 ($C_2H_5Cl^{37+}$)}. The variations in the ionic current intensity correspond to the temperature ranges over which the loss in weight is recorded in the TG curve.

Complexes containing both the chloride and bromide ligands in the coordination sphere of manganese(II) release simultaneously Et_3N, EtCl and EtBr during decomposition as evidenced by variations in the ionic currents of the m/z values of 26 ($C_2H_2^+$), 27 ($C_2H_3^+$), 28 ($C_2H_4^+$), 29 ($C_2H_5^+$), 30 ($C_2H_6^+$), 49 (CH_2Cl^{35+}), 58 ($C_3H_8N^+$), 64 ($C_2H_5Cl^{35+}$), 66 ($C_2H_5Cl^{37+}$), 86 ($C_5H_{12}N^+$), 100 ($C_6H_{14}N^+$), 101 ($C_6H_{15}N^+$), 108 ($C_2H_5Br^{79+}$) and 110 ($C_2H_5Br^{81+}$).

The presence of these volatiles released during thermal decomposition of bis(tetraethylammonium) tetrahalogenomanganates(II) has also been confirmed by the FTIR spectra. For instance, in a FTIR spectrum of the volatiles from $(Et_4N)_2[MnCl_4]$, bands were recorded around 660 cm^{-1} (ν C–Cl), 740–1210 cm^{-1} (δ C–C–H), 1290–1390 cm^{-1} (δ H–C–N), 1470 cm^{-1} (δ H–C–H) and 2800–2980 cm^{-1} (ν C–H). These bands are compatible with those of the theoretical IR spectra of ethylamine and ethyl chloride (Fig. 4).

Formation of the volatiles containing halogen ions triggers some changes in the coordination sphere of Mn(II). In the Far-FTIR spectrum of $(Et_4N)_2[MnCl_4]$ there are bands assigned to bending vibrations of Cl–Mn–Cl (at 79 and 118 cm^{-1}) and to the stretching ones of Mn–Cl at 282 cm^{-1}. These bands are absent in the spectrum of the sinter, this indicating destruction of the tetrahedral geometry of the manganese(II) complex upon heating up to 648 K.

Juxtaposition of the spectra of the sinters obtained at 648 K (first step) and 693 K (second step), represented in Fig. 5(2) and (3), resp., reveals that they have a similar structural unit. For comparison of the band frequencies, a standard spectrum of anhydrous manganese(II) chloride has been recorded (Fig. 5(1)).

A closer inspection of the position and relative intensities of the absorption bands in the spectra represented in Fig. 5 shows that the

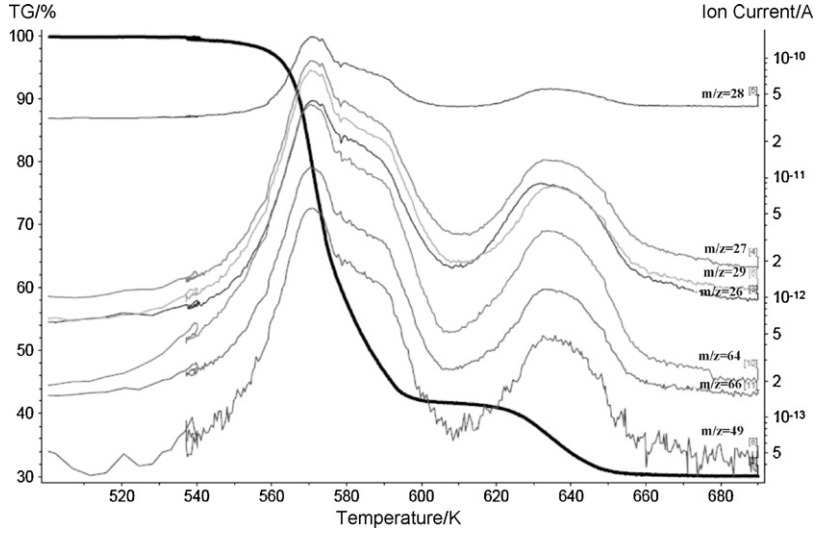

Fig. 3. TG curve of $(Et_4N)_2[MnCl_4]$ ($\beta = 1$ K/min over the range 523–723 K) and ionic currents for m/z assigned to EtCl recorded during decomposition of the complex.

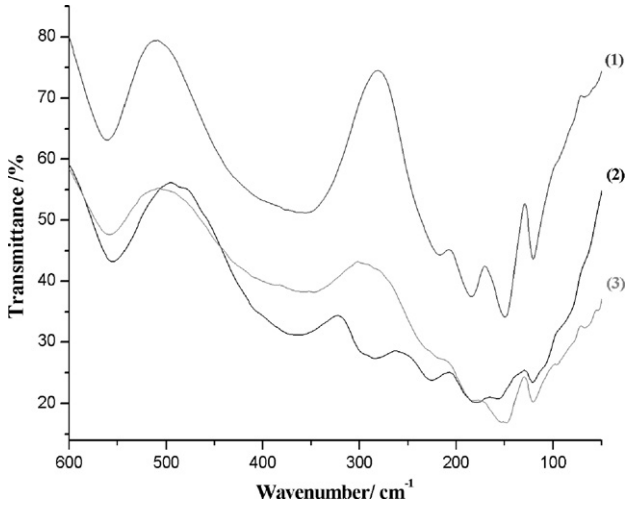

Fig. 5. Far-FTIR spectra of the $(Et_4N)_2[MnCl_4]$ sinters obtained at 648 K **(2)** and 693 K **(3)**, and the spectrum of $MnCl_2$ **(1)**.

product of the first (648 K) and second (693 K) decomposition steps of $(Et_4N)_2[MnCl_4]$ is $MnCl_2$. Also the X-ray diffraction results show that $MnCl_2$ is one of the crystalline phases present in the sinter. As can be seen in Fig. 6, part of the XRD reflexes of the sinter left after combustion of $(Et_4N)_2[MnCl_4]$ at 693 K may be attributed to $MnCl_2$.

Manganese(II) chloride was also found at the second step of decomposition of $(Et_4N)_2[MnBrCl_3]$ as indicated by the position of relative band intensities in the Far-FTIR spectrum of a sinter obtained at 703 K.

The difference in the thermal decomposition patterns of the $(Et_4N)_2[MnBr_nCl_{4-n}]$ compounds is due to the fact that $MnCl_2$ left at the first step of decomposition of $(Et_4N)_2[MnCl_4]$, $(Et_4N)_2[MnBrCl_3]$ and $(Et_4N)_2[MnBr_2Cl_2]$ probably reacts with Et_3N being released to form an $Et_3N{:}MnCl_2$ adduct which undergoes thermal decomposition during the next step. This can be seen at a slow rate of temperature increase (Fig. 7). A slower diffusion of the gases (at $\beta = 1$ K/min) from the sample facilitates formation of the $Et_3N{:}MnCl_2$ adduct which undergoes decomposition at higher temperature to release Et_3N.

Knowledge of the volatile and solid decomposition products of $(Et_4N)[MnBr_nCl_{4-n}]$ ($n = 0$–2) allows the following pathway of the first step of decomposition of the compound to be suggested:

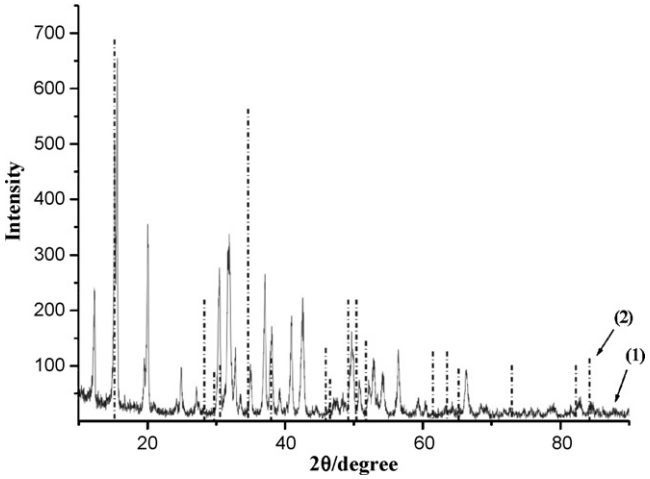

Fig. 6. X-ray diffraction pattern of the sinter left after combustion of $(Et_4N)_2[MnCl_4]$ at 693 K (second decomposition step) together with X-ray reflexes assigned to $MnCl_2$.

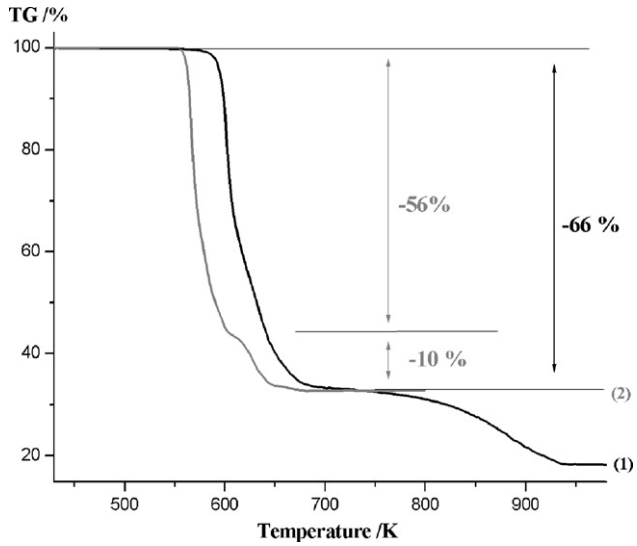

Fig. 7. TG curves of $(Et_4N)_2[MnBrCl_3]$, $\beta = 15$ K/min **(1)** and 1 K/min **(2)**, in argon.

$$(Et_4N)_2[MnCl_4] \xrightarrow[\text{-}Et_3N,\ EtCl]{\text{ok. 573 K}} Et_3N{:}MnCl_2,\ MnCl_2,\ C_xH_yN_z \xrightarrow[\text{-}Et_3N]{\text{ok. 643 K}} MnCl_2,\ C_xH_yN_z$$

The loss in weight due to formation of $MnCl_2$ during the first two decomposition steps (72%, TG curve, Table 2) is compatible with the theoretical one (72%). This indicates a total release of the organic fragment as Et_3N and EtCl. However, in the final decomposition product, non-decomposed organic matter ($C_xH_yN_z$) has been found.

Analogous decomposition pattern can also be suggested for $(Et_4N)_2[MnBrCl_3]$:

$$(Et_4N)_2[MnBrCl_3] \xrightarrow[\text{-}EtCl,\ EtBr]{\text{ok. 553 K}} Et_3N{:}MnCl_2,\ MnCl_2,\ C_xH_yN_z \xrightarrow[\text{-}Et_3N]{\text{ok. 733 K}} MnCl_2,\ C_xH_yN_z$$

Here, the calculated loss in weight due to formation of $MnCl_2$ is 74%. On the other hand, that taken from the TG curve is smaller (66%, Table 2, Fig. 7). This difference can be attributed to the formation of $MnBr_2$ as well. Assuming that during the second step equimolar quantity of $MnCl_2$ and $MnBr_2$ is being formed, the theoretical loss in weight would be just 66%. However, the presence of $MnBr_2$ in the residue (703 K) has been ruled out by its Far-FTIR spectrum whose shape suggests that $MnCl_2$ is the sole decomposition product. It can thus be concluded that the smaller than theoretical loss in weight can be explained in terms of the presence of the non-decomposed organic matter. Its presence would also affect the course of the final decomposition step of the compound.

The most intricate decomposition pattern among the $(Et_4N)_2[MnBr_nCl_{4-n}]$ ($n = 0$–2) compounds has been exhibited

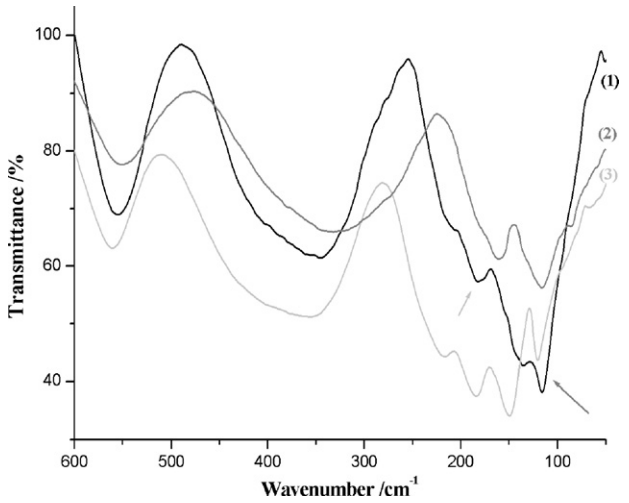

Fig. 8. Far-FTIR spectrum of the sinter of $(Et_4N)_2[MnBr_2Cl_2]$ left at 693 K **(1)** superimposed with those of $MnBr_2$ **(2)** and $MnCl_2$ **(3)**.

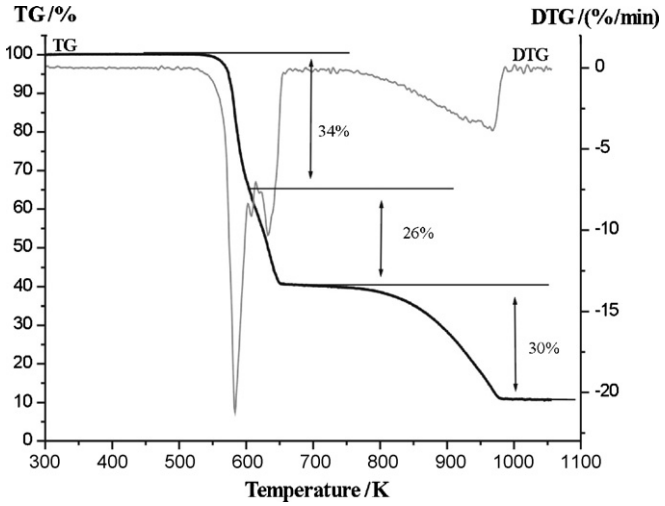

Fig. 9. TG and DTG curves of $(Et_4N)_2[MnBr_3Cl]$, β = 15 K/min, in argon.

by $(Et_4N)_2[MnBr_2Cl_2]$. A sinter left at 693 K (second decomposition step) has been shown to contain both $MnCl_2$ and $MnBr_2$. In its Far-FTIR spectrum (Fig. 8) bands at identical positions to those of $MnBr_2$ (gray arrow) and $MnCl_2$ (light gray arrow) have been found. An additional proof in favour of those halides is an X-ray diffraction pattern of the sinter in which the most intense peaks correspond to X-ray reflexes of $MnCl_2$ and $MnBr_2$.

The loss in weight in the TG curve (66%) corresponds roughly to an equimolar mixture of $MnCl_2$ and $MnBr_2$ (69%). On this basis the following pathway can be suggested for the first two decomposition steps of $(Et_4N)_2[MnBr_2Cl_2]$:

$$\mathbf{(Et_4N)_2[MnBr_2Cl_2]}$$

$$\xrightarrow[-EtCl,\ EtBr]{-Et_3N,\ \text{ok. 550 K}}$$

$$\mathbf{Et_3N{:}MnCl_2,\ MnCl_2,\ MnBr_2,\ C_xH_yN_z}$$

$$\xrightarrow{-Et_3N,\ \text{ok. 630 K}}$$

$$\mathbf{MnCl_2,\ MnBr_2,\ C_xH_yN_z}$$

Slightly different are the decomposition patterns of complexes with a higher number of bromide ligands. Thus, the nature of ligands in the coordination sphere of manganese(II) has an influence on the character of thermal transformations of the bis(tetraethylammonium) tetrahalogenomanganates(II).

The shapes of the TG curves of $(Et_4N)_2[MnBr_3Cl]$ (Fig. 9) and $(Et_4N)_2[MnBr_4]$ suggest a two-step decomposition of the compounds.

The clear-cut extrema in the DTG curves corresponding to the first step of decomposition indicate two separate reactions to occur. During those two steps, identical volatiles were released as indicated by variations in the ionic current intensities for the same m/z values. During decomposition of $(Et_4N)_2[MnBr_3Cl]$ and $(Et_4N)_2[MnBr_4]$, Et_3N, EtCl and EtBr as well as Et_3N and EtBr, respectively, were formed.

Due to high transformation rate taking place and consecutive reactions, it was difficult to collect samples during the first step of decomposition. Heating of $(Et_4N)_2[MnBr_3Cl]$ up to 613 K gave a sinter whose Far-FTIR spectrum allowed only to rule out the presence of either manganese(II) halide. A comparison of the Far-FTIR spectrum of $(Et_4N)_2[MnBr_3Cl]$ and of its sinter reveals some changes in the coordination sphere of the Mn(II) ion. Thus, the intensity of the stretching vibrations of Mn–Br decreases while that of Mn–Cl disappears. There are also changes over the range of the bending vibrations of Br–Mn–Br.

Manganese(II) bromide is the product of the next step of decomposition of $(Et_4N)_2[MnBr_3Cl]$ and $(Et_4N)_2[MnBr_4]$, at 663 K. This conclusion is based on similarity of the Far-FTIR spectra of the corresponding sinters and anhydrous manganese(II) bromide as well as the X-ray diffraction patterns of the samples.

A careful scrutiny of the results of experiments with this class of compounds revealed a difference between the decomposition patterns of $(Et_4N)_2[MnCl_4]$, $(Et_4N)_2[MnBr_3Cl]$ and $(Et_4N)_2[MnBr_2Cl_2]$ on the one hand, and the remaining two bis(tetraethylammonium) tetrahalogenomanganates(II), $(Et_4N)_2[MnBrCl_3]$ and $(Et_4N)_2[MnBr_4]$, on the other hand. During thermal decomposition of the first-named compounds, $MnCl_2$ is left at the first step which subsequently forms a stable $Et_3N{:}MnCl_2$ adduct. With the two last-named compounds, initially only small changes take place in the coordination sphere of Mn(II), and $MnBr_2$ is formed at the next step. Furthermore, $MnBr_2$, in contrast to $MnCl_2$, does not react wit the volatiles Et_3N. The poorer capacity of $MnBr_2$ to form adducts can be due to a lower electronegativity of bromine as compared to that of chlorine on the one hand, and to the steric hindrance of the former, on the other hand. The more electronegative chlorine atom increases the positive charge on the metal cation to enhance its interaction with the lone electron pair on the nitrogen atom of the triethylamine molecule.

As the compiled results do not warrant certainty as to the chemical composition of the first decomposition product ("?" in the scheme), it is rather difficult to write a stoichiometric equation for the processes progressing during the first step of the thermal dissociation. This notwithstanding, having in hand composition of the released gases and of the solid product of the second step, the following scheme can be suggested for the first two steps of the decomposition of $(Et_4N)_2[MnBr_3Cl]$:

$$\mathbf{(Et_4N)_2[MnBr_3Cl]}$$

$$\xrightarrow[-EtCl,\ EtBr]{-Et_3N,\ \text{ok. 563 K}}$$

$$\mathbf{?}$$

$$\xrightarrow[-EtCl,\ EtBr]{-Et_3N,\ \text{ok. 610 K}}$$

$$\mathbf{MnBr_2,\ C_xH_yN_z}$$

and, by analogy, for $(Et_4N)_2[MnBr_4]$:

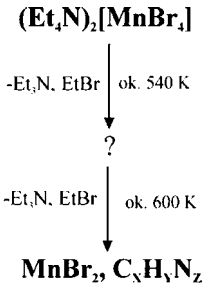

The loss in mass in the TG curve of $(Et_4N)_2[MnBr_3Cl]$ assigned to the formation of $MnBr_2$ is 61% (Table 2, Fig. 9), whereas the theoretical one is 63%. With $(Et_4N)_2[MnBr_4]$ respective losses are 60% (Table 2) and 66%. The differences are most probably due to non-decomposed organic cations of the compounds, $C_xH_yN_z$.

Irrespective of the identity of anion, the final step of the thermal decomposition of the bis(tetraethylammonium) tetrahalogenomanganates(II) leaves identical product, manganese(II) halide. This, being the solid product of the last but one step undergoes conversion to manganese(II) carbide and small amounts of elemental manganese. The presence of the latter in sinters obtained around 1000 K has been confirmed by X-ray diffraction patterns. A similar result was previously reported for the $(Bu_4N)_2[MnBr_nCl_{4-n}]$ (n = 0–4) counterparts [14].

The final step of the thermal decomposition of the compounds is not quite clear. Without any doubt, the final decomposition products are manganese carbides. Unfortunately, it is difficult to precisely determine their composition solely on the basis of X-ray analysis of the polycrystalline samples. The products may be either a carbide of definite composition or a mixture of carbides. There are five manganese carbides described in the literature, namely $Mn_{15}C_4$, $Mn_{23}C_6$, Mn_3C, Mn_5C_2, and Mn_7C_3 [19,20].

There are also some difficulties in the identification of the volatiles undoubtedly released at that step (see loss in weight in the TG curve). Most probably these are inorganic compounds and this makes the FTIR spectral analysis difficult. Identification of the gases could be possible from analysis of variations in the intensities of the ionic currents. However, the variations are missing for the m/z values corresponding to Cl_2, Br_2, HCl and HBr. This indicates that either the products are not released at all during thermal degradation of a manganese(II) halide or their concentration is too low to be recorded by the detector. It can also be speculated that the halide ions react with the incompletely combusted organic residue, $C_xH_yN_z$, to form intricate systems. The residue is also a source of carbon for the manganese carbides being formed. Furthermore, decomposition of the residue at high temperature (around 1000 K) can afford elemental carbon which subsequently can reduce manganese(II) to elemental manganese that can be seen with naked eye both in the combusted samples as well as in the X-ray diffraction patterns.

A comparison of the results published previously [14] with those presented here shows that the decomposition process of a compound depends also on the identity of cation. Thus the shapes of the TG curves of $(Et_4N)_2[MnCl_4]$ and $(Bu_4N)_2[MnCl_4]$ show unambiguously that the size of the cation has an influence on both the decomposition point and the number of decomposition steps. The bulkier the cation is, the lower the decomposition point of the complex becomes. This finding can be interpreted in terms of reasoning that an increase in the cation size results in an increase in interionic space. This, in turn, results in lowering crystal lattice energy of a salt.

4. Conclusions

The bis(tetraethylammonium) tetrahalogenomanganates(II) undergo, as a rule, reversible phase transformations associated with small movements of ions. It should be emphasized that the compounds do not melt. Decomposition of the complexes takes place in the solid phase in two or three steps depending on the identity of the anion. Compounds with identical tetraethylammonium cation are characterized by comparable decomposition points and release similar volatile products. In the case of $(Et_4N)_2[MnBr_nCl_{4-n}]$ these are ethyl halides and triethylamine. However, both the nature of the ligand in the coordination sphere of manganese(II) and the size of the organic cation have a significant influence on temperature and character of the thermal transformations of the compounds. Decomposition of $(Et_4N)_2[MnCl_4]$, $(Et_4N)_2[MnBrCl_3]$ and $(Et_4N)_2[MnBr_2Cl_2]$ results in a stable adduct, $Et_3N{:}MnCl_2$, formed at the first step. This adduct is analogous to $Bu_3N{:}MnCl_2$ formed at the second step of decomposition of $(Bu_4N)_2[MnCl_4]$ and $(Bu_4N)_2[MnBrCl_3]$ [14]. The two remaining compounds, $(Et_4N)_2[MnBr_3Cl]$ and $(Et_4N)_2[MnBr_4]$ leave behind only a manganese(II) halide during the second step. However, irrespective of the nature of the organic cation or complex anion, the final step of thermal decomposition of the bis(tetralkylammonium) tetrahalogenomangananates(II) affords identical products. A manganese(II) halide, being the solid product of the last but one decomposition step of the compounds undergoes conversion to a manganese carbide and small amounts of elemental manganese.

The results of this contribution, as compared to those previously reported for compounds of general formula $(Et_4N)_2[MBr_nCl_{4-n}]$, where M = Fe, Co, Cu; n = 0–4 [11–13] reveal the influence of the central ion identity on the course of thermal decomposition of the complexes. Only during decomposition of compounds of the least electronegative element, manganese(II), stable adducts are formed between the solid $MnCl_2$ and the volatile amines, Et_3N and Bu_3N. Finally, depending on the identity of the metal, the final products of the thermal decomposition in an inert atmosphere are metal carbides and/or elemental metal.

Acknowledgement

This research was supported by the Polish State Committee for Scientific Research under grant DS/8232-4-0088-9.

References

[1] P. Day, M. Kurmoo, T. Mallah, I.R. Marsden, R.H. Friend, F.L. Pratt, W. Hayes, D. Chasseau, J. Gaultier, G. Bravic, L. Ducasse, J. Am. Chem. Soc. 114 (1992) 10722–10729.
[2] H. Kobayashi, H. Cui, A. Kobayashi, Chem. Rev. 104 (2004) 5265–5288.
[3] T. Enoki, A. Miyazaki, Chem. Rev. 104 (2004) 5449–5477.
[4] E. Coronado, P. Day, Chem. Rev. 104 (2004) 5419–5448.
[5] T. Mori, H. Inokuchi, Bull. Chem. Soc. Jpn. 61 (1988) 591–593.
[6] S. Hebrard, G. Bravic, J. Gaulteier, D. Chasseau, Acta Cryst. C 50 (1994) 1892–1894.
[7] G. Guionneau, G. Bravic, J. Gaultier, D. Chasseau, M. Kurmoo, D. Kanazawa, P. Day, Acta Cryst. C 50 (1994) 1894–1896.
[8] T. Naito, T. Inabe, K. Takeda, K. Awaga, T. Akutagawa, T. Hasegawa, T. Nakamura, T. Kakiuchi, H. Sawa, T. Yamanoto, H. Tajima, J. Mater. Chem. 11 (2001) 2221–2227.
[9] W. Xu, R. Shen, C.-M. Liu, D. Zhang, D. Zhu, Synth. Met. 133–134 (2003) 349–351.
[10] F. Zhao, P. Li, X. Zhu, L. Dong, Acta Cryst. E 64 (2008) m1516.
[11] E. Styczeń, Z. Warnke, D. Wyrzykowski, Thermochim. Acta 454 (2007) 84–89.
[12] E. Styczeń, W.K. Jóźwiak, M. Gazda, D. Wyrzykowski, Z. Warnke, J. Therm. Anal. Cal. 91 (2008) 979–984.
[13] E. Styczeń, A. Pattek-Janczyk, M. Gazda, W.K. Jóźwiak, D. Wyrzykowski, Z. Warnke, Thermochim. Acta 480 (2008) 30–34.
[14] E. Styczeń, D. Wyrzykowski, M. Gazda, Z. Warnke, Thermochim. Acta 481 (2009) 46–51.

[15] N.S. Gill, R.S. Nyholm, J. Chem. Soc. (1959) 3997–4007.
[16] ICDD PDF-2 Database Release 1998, ISNN 1084-3116.
[17] T.P. Melia, R. Merrifield, J. Inorg. Nucl. Chem. 32 (1970) 1873–1876.
[18] M. Sawicka, P. Storoniak, J. Błażejowski, J. Rak, J. Phys. Chem. A 110 (2006) 5066–5074.
[19] R. Kononov, O. Ostrovski, S. Ganguly, Metall. Mater. Trans. B 39 (2008) 662–668.
[20] N.N. Greenwood, A. Earnshaw, Chemistry of the Elements, Pergamon Press, Oxford, 1990.